DOI: 10.1002/ ((please add manuscript number))
Article type: Full Paper

Enhancing Photovoltaic Performance of Aromatic Ammonium based Two-Dimensional Organic-Inorganic Hybrid Perovskites via Tuning CH···π Interaction

*Liang Yan, Jun Hu, Ninghao Zhou, Andrew M. Moran, Wei You**

Dr. Liang Yan, Dr. Jun Hu, Ninghao Zhou, Prof. Andrew M. Moran, Prof. Wei You
Department of Chemistry, University of North Carolina at Chapel Hill, Chapel Hill, North Carolina 27599, United States
E-mail: wyou@unc.edu

Keywords: 2D organic inorganic hybrid perovskite, solar cell, CH···π interaction

Abstract: Phenethylammonium (PEA) based 2D perovskite is an interesting example of 2D perovskites, serving as the gateway towards further introduction of functional conjugated organic cations into 2D perovskites for a variety of applications, for example, photovoltaics. However, the efficiency of photovoltaic devices based on PEA 2D perovskites only achieved ~ 7% for <n>=3, significantly lower than what have been achieved for other cations based 2D perovskites. Here we show that, by introducing propyl ammonium (C3A) into the PEA based 2D perovskites, the device efficiency can be improved to ~10% for 1:1 C3A:PEA based 2D perovskites (<n>=3). Further investigation discloses that, tuning the CH···π interaction (between C3A and PEA or between two PEA) can have multiple beneficial impacts on such modified 2D perovskites, including (a) removal of undesirable *n*=1 phase, (b) lowering the density of trap states, and (c) achieving rather large crystalline grains. Additionally, when substituting with 50% C3A, other aromatic ammonium cations based 2D perovskites (<n>=3) also witness similar efficiency enhancement in their photovoltaic devices, boasting the general use of such method. Our results highlight that, the strategic tuning of non-covalent

interactions (such as the CH···π interaction) is a viable and important method in further developing 2D perovskites for photovoltaics.

1. Introduction

Though structurally closely related to three-dimensional (3D) perovskites (e.g., $CH_3NH_3PbI_3$, MAPI), two-dimensional (2D) Ruddlesden-Popper type perovskites – with a formula of $A_2B_{n-1}Pb_nI_{3n+1}$ – have their own unique properties,[1-3] due to the incorporation of large organic cations that separate the metal halide octahedra layer (e.g., PbI_6^{4-}). Generally, A stands for the large spacer cations, B is usually a small cation such as methylammonium (MA), formamidinium (FA) or Cs^+, and *n* is the number of metal halide octahedra layers between the organic cation spacer layers. Though in principle, *n* could be any integer, here we limit *n* to small values ($n \leqslant 5$) for 2D or quasi-2D perovskites since for $n > 5$, the '2D' perovskites are much more similar to quasi-3D structures.[1]

The rising interest for 2D perovskites perhaps comes from their inherently better stability than that of 3D perovskites, mainly due to the large formation energy of these 2D perovskites.[4] Thus many research groups have attempted to apply 2D perovskites to passivate either the surface or grain boundaries of 3D perovskites,[5, 6] aiming to achieve better stability while maintaining desirable properties of the original 3D perovskites, e.g., high photovoltaic (PV) efficiency. In addition, the unique quantum well structure of 2D perovskites and chemical adjustability of organic cations offer prospects for other applications, such as light emitting diode (LED),[7, 8] field-effect transistor (FET),[9-12] among others.[1, 13]

Directly applying 2D perovskites for solar cells has met a serious challenge however, since their layer structures tend to adopt a parallel orientation to the substrate and these insulating organic spacer cations (A in $A_2B_{n-1}Pb_nI_{3n+1}$) would prevent charge transport perpendicular to the substrate.[14] A breakthrough emerged in 2016, when Tsai et al. introduced a hot casting method,[15] which appears to re-align the metal halide octahedra layer to be perpendicular to the substrate, thereby leading to an observed efficiency as high at

12.5% and much improved stability. Since then, much more progress has been made in the development of 2D or quasi 2D perovskites ($n \leqslant 5$) for solar cells.[16-21] Among all these studies, the most commonly used large organic spacer cations are butylammonium (BA) and phenethylammonium (PEA).[22] By mixing with other cations [23-27] or using additive such as NH_4SCN,[19, 28, 29] NH_4Cl[19] or MACl,[30] the PV efficiency has been further improved to close to 15% in BA or PEA based 2D perovskite solar cells.[19, 24, 25] Without mixing cation or using additive, BA based 2D perovskite solar cells can achieve relatively better efficiency, ~ 12% for <n>=4 and 11% for <n>=3;[15] in contrast, PEA based systems only achieved ~ 7% for <n>=3 and ~ 9% for <n>=4.[31] However, PEA based 2D perovskites are more interesting from the perspective of introducing large functional conjugated organic cations into 2D perovskites, [32] since PEA is perhaps the smallest conjugated cation.

Performance of 2D perovskite solar cells can be affected by many factors, including surface morphology, phase composition, phase distribution and crystal orientation of the perovskite films.[31] For PEA based 2D perovskite solar cells, there are two outstanding issues that limit the device efficiency. First, PEA based 2D perovskite films always have a significant amount of the n=1 phase which has the largest band gap among all phases typically co-existing in 2D perovskite films and the slowest charge transport.[33] The limited absorption due to a large band gap, together with the slow charge transport, contribute significantly to the observed low power conversion efficiency for PEA based 2D perovskite solar cells. Therefore, reducing or even eliminating the amount of n=1 phase would be beneficial to the further improvement of 2D perovskite based solar cells. Second, the larger size of PEA could lead to more defects in the crystals, and therefore, more traps in the perovskite films; these traps act as charge recombination centers, causing a poor fill factor (FF). Thus, reducing the amount of traps is also important for device performance.

It has been shown that adjusting the intermolecular interaction between organic cations in 2D/quasi 2D perovskites can have significant impact on the phase distribution, crystal

orientation and surface morphology.[34, 35] Explored intermolecular interactions include the van der Waals interaction, aryl-perfluoroaryl interaction, and hydrogen bonding.[24, 34, 36-38] Promising results have been obtained. For example, we have recently discovered that the quasi 2D perovskite based solar cells with added perfluoro-phenethylammonium (F5-PEA) could significantly improve their stability while maintaining decent efficiency,[34] where the non-covalent interaction between PEA and F5-PEA has been identified as the key reason.

CH···π interaction is another strong, yet less explored (inter)molecular interaction,[39] which has never been investigated in 2D/quasi 2D perovskites. During our ongoing investigation on tuning intermolecular interactions in 2D/quasi 2D perovskites, we find that the CH···π interaction could be utilized to tune the compositions of different phases in PEA based 2D perovskites. Specifically, replacing 50% of PEA cations with propylammonium cations (C3A) in the PEA based 2D perovskites (<n>=3) can selectively remove *n*=1 phase. Furthermore, the C3A cations could passivate the defects (trap states) in PEA based 2D perovskite film, likely due to the small size of C3A. Both effects – controlling phase composition and passivating the defects – enhanced the device efficiency of PEA based 2D perovskite (<n>=3) solar cells to the level of 10% with a 1:1 ratio of PEA:C3A. In contrast, the original PEA based 2D perovskites solar cell only afforded an efficiency of ~ 7.5%. Furthermore, these beneficial effects from C3A appear to be generally applicable to other aryl derived cations based 2D perovskites; specifically, we have observed efficiency enhancement for 2D perovskite solar cells based on thiophenethylammonium (TEA), 2-fluorophenethylammonium (oFPEA) or 3-fluorophenethylammonium (mFPEA).

2. Results and Discussion

2.1. Spectroscopic evidence for phase control via substituting PEA with C3A

Our original intention was to utilize a cation of small size to fill/passivate the trap states in PEA based 2D perovskites, aiming to improve the device performance.[26, 27] In this regard,

ethyl ammonium (C2A) would be a good choice; however, its small size would enable its incorporation into the PbI_2 layer [40, 41], leading to 3D perovskites. Thus we chose propyl ammonium (C3A), the smallest alkyl cation that can form 2D perovskites structure.[42] However, C3A might still introduce complications, since this cation can form not only normal Ruddlesden-Popper (RP) 2D perovskites[42] but also other type of perovskites.[40, 43, 44] Yet the XRD patterns for our C3A incorporated perovskites (*vide infra*) are different from these of other type of perovskite published; [40, 43, 44] together with other evidences (*vide infra*), we believe the perovskites studied in here still belong to RP 2D perovskites. Nevertheless, as we will show below, the incorporation of C3A into PEA based 2D perovskites not only passivates the defects, furthermore, it can selectively remove the undesirable *n*=1 phase.

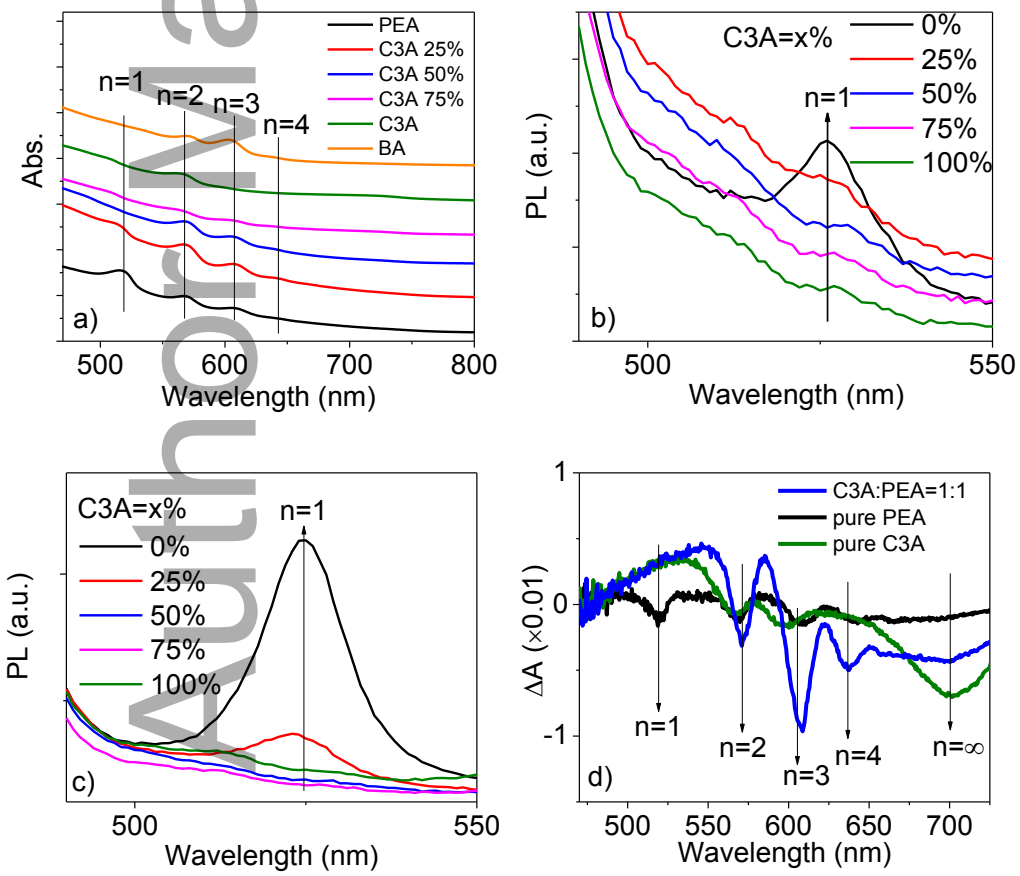

Figure 1. a) Absorption profiles of PEA, C3A, BA and C3A:PEA mixed cations based perovskite with <n>=3, **b)** PL of front side (air) and **c)** back side (glass) of 2D perovskite with different C3A and PEA ratios, **d)** TA of 2D perovskite film of pure PEA, pure C3A and C3A:PEA=1:1 with <n>=3 at delay time 1 ps.

As shown in **Figure 1a)**, the PEA based 2D perovskite (<n>=3) film exhibits a rather strong *n*=1 absorption peak, contrasting the negligible *n*=1 absorption in BA based (<n>=3) film. Since the *n*=1 phase has the largest band gap and lowest conductivity among all different *n* phases in 2D perovskites, ideally one should eliminate the *n*=1 phase if these perovskites are intended for photovoltaic applications. Interestingly, after substituting C3A into PEA based 2D perovskites (<n>=3), i.e., replacing PEA with equal moles of C3A to maintain the average film composition (<n>=3), the absorption intensity of the *n*=1 phase gradually reduces (**Figure 1a**) as the amount of C3A increases, and completely vanishes at 50% substitution of C3A (C3A:PEA=1:1). Further increasing the amount of C3A (i.e., 75%) results in the absorption profile closer to that of the pure C3A based 2D perovskites (**Figure 1a**), where the absorption of different *n* phases becomes rather weak.

Since photoluminescence (PL) can be used to identify the phase composition and distribution,[20, 31] we further measured the PL of our 2D perovskites (<n>=3) on glass substrate from both the back side and the front side to further confirm the impact of introducing C3A. At 0% C3A, one can clearly observe the strong PL signal for *n*=1 phase from both sides of the film (**Figure 1b** and **Figure 1c**). As C3A amount increases, the PL from *n*=1 phase weakens and eventually disappears; this happens at 25% C3A for the PL measured from the front side and 50% C3A for the PL measured from the back side. Thus, these PL data support the discovery from the UV-Vis measurement, i.e., substituting PEA with C3A can selectively remove the *n*=1 phase in PEA based 2D perovskites. Further evidence on the selective removal of *n*=1 phase by adding C3A comes from transient absorption (TA) measurement, a technique that has been used to identify the composition in 2D perovskite thin film.[45] Shown in **Figure 1d**, the TA signal for *n*=1 phase can be clearly identified for pure PEA based 2D perovskites (with just 1 ps after pump excitation); in contrast, this signal disappears for the film with 50% C3A (i.e., C3A:PEA=1:1).

2.2. Confirming interaction with model compounds (*n*=1) of different C3A:PEA ratio

To understand why substituting PEA with C3A leads to the selective removal of *n*=1 phase in PEA based <n>=3 perovskite films, we next investigated perovskites films of *n*=1, which would allow to focus on the interactions between C3A and PEA in the organic cation layer between lead iodide octahedra layers. **Figure 2a** shows that the absorption of the 50% C3A substitution (i.e., C3A:PEA=1:1) has a distinctively different exciton peak compared with those of 0% and 100% C3A (i.e., pure PEA and pure C3A based perovskite film of *n*=1, respectively), indicating the presence of a new 2D perovskite phase for 50% C3A, likely due to the interaction between C3A and PEA in the organic interlayer. This new phase from the C3A:PEA (1:1) base 2D perovskite film (*n*=1) can still be observed from the 25% C3A based film, which has two absorption peaks, appearing to be a superposition of the absorption from 50% C3A and 0% C3A (i.e., pure PEA). On the other hand, the absorption spectrum of 75% C3A based film is very similar to that of 100% C3A (i.e., pure C3A). These observations imply that further increasing the content of C3A beyond 50% could lead to disruption of the formation of C3A:PEA (1:1) perovskite phase.

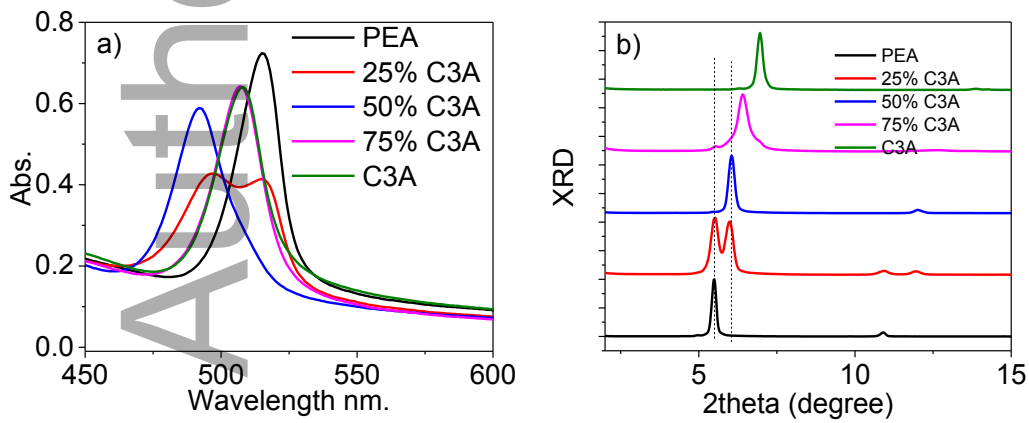

Figure 2. a) Absorption profiles and b) small angle range of XRD of C3A:PEA based 2D perovskite with *n*=1.

Characterization of all these *n*=1 films with powder X-ray diffraction (XRD) offers further evidence on the formation of the C3A:PEA (1:1) perovskite phase. For example, the XRD patterns in the small angle range (**Figure 2b**) clearly indicate that the 25% C3A based film contains the original PEA phase (i.e., 0% C3A) and a new phase corresponding to the C3A:PEA (1:1) perovskite. On the other hand, the small angel peak for the 75% C3A based film contains contributions from 0%, 50%, and 100% C3A based perovskite phases, resulting in the broadening of this peak and shifting in position. It appears that the 75% C3A based perovskite film (*n*=1) has significant amount of structural disorder, as further indicated by the rather broadened peaks in its XRD pattern in large angle range (**Figure S3**).

Taking all these results together, we propose that there is a strong interaction between C3A and PEA, likely through the CH···π interaction, which would account for the observed new perovskite phase in C3A:PEA (1:1) based film (*n*=1) and the selective removal of the *n*=1 phase in PEA based 2D perovskite film (<n>=3) with 50% C3A substitution. Indeed, it has been well studied that there is a strong CH···π interaction between the methyl group and the benzene ring.[46-48] In our study, there should be no CH···π interaction in pure C3A based 2D perovskite films, because there are no π delocalized structures in the organic interlayers. In contrast, there is (sp^2) CH···π interaction in pure PEA based 2D perovskite films, evidenced by analyzing the crystal structure of PEA_2PbI_4 (*n*=1).[49] Specifically, in its crystal structure (**Figure S5**), the smallest C-C distances between the benzene rings are 3.896Å and 3.846Å, the corresponding H-C distances between adjunct benzene rings are about 3.047Å and 3.008Å, which are in the range of the intermolecular CH···π interaction (3.05Å).[50] And further calculation about the angle and distance between the CH and π plane indicates the CH···π interaction exists in PEA_2PbI_4 according to the CH···π model by Nishio,[51] as shown in **Table S1**.

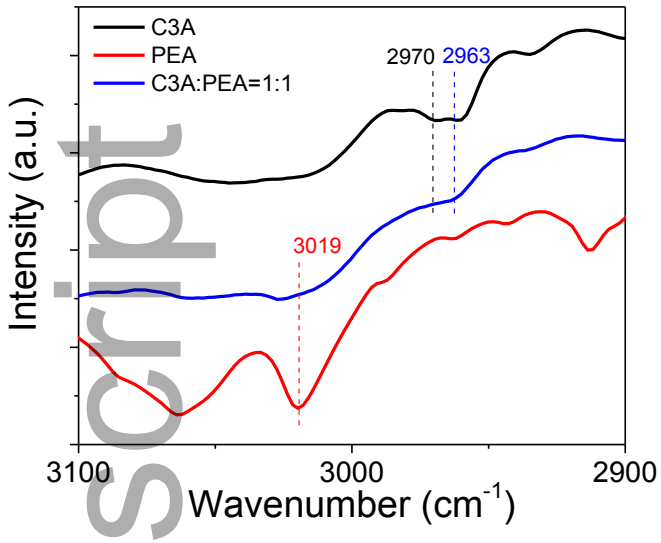

Figure 3. FT-IR spectrum of perovskite film with *n*=1 based on pure C3A, pure PEA and C3A:PEA=1:1 mixture.

Further evidence for the proposed CH···π interaction in our 2D perovskites comes from Fourier-transform infrared (FTIR) study of these perovskite films (*n*=1). It is known that for intermolecular CH···π interaction, there is a small shift to lower frequency for the C-H stretching band in the FTIR spectrum.[50] As shown in **Figure 3**, the sp^3 C-H stretching band for the methyl group in C3A (based perovskite film) shifts from 2970 cm^{-1} (for pure C3A, *n*=1) to 2963 cm^{-1} (for C3A:PEA = 1:1, *n*=1),[52] indicating the intermolecular sp^3 CH···π interaction between the methyl group in C3A and the benzene π ring in PEA. On the other hand, sp^2 C-H stretching for the benzene ring in PEA (based perovskite film) is located at 3019 cm^{-1} (for pure PEA, *n*=1), which almost disappears for 50% C3A based film (C3A:PEA = 1:1, *n*=1). This indicates that the intermolecular CH···π interaction between the methyl group in C3A and the benzene π ring in PEA, has largely replaced the previously existing PEA-PEA (CH···π) interaction in pure PEA based perovskites (*n*=1), given the 1:1 ratio of C3A to PEA. [39, 47, 53]

All these observations strongly support the proposed CH···π interaction between the methyl group in C3A and the benzene π ring in PEA, in these mixed cations based 2D perovskite films (n=1). For the 2D perovskite films (<n>=3), the clear observation of n=1 phase for pure PEA based one is likely caused by the strong (sp^2) CH···π interaction between PEA molecules; similarly, no n=1 phase was observed for pure C3A based one can be ascribed to the absence of CH···π interaction. As for the absence of n=1 phase in the 1:1 mixed C3A and PEA based 2D perovskites, we argue that the sp^3 CH···π interaction between the C3A and PEA is not strong enough to maintain the n=1 phase. These results indicate that the CH···π interaction can play an important role in the phase formation in 2D perovskites; adjusting the CH···π interaction can be utilized to fine tune the phase composition in these 2D perovskite films.

2.3. Photovoltaic device performance of 2D perovskites of different C3A:PEA ratio

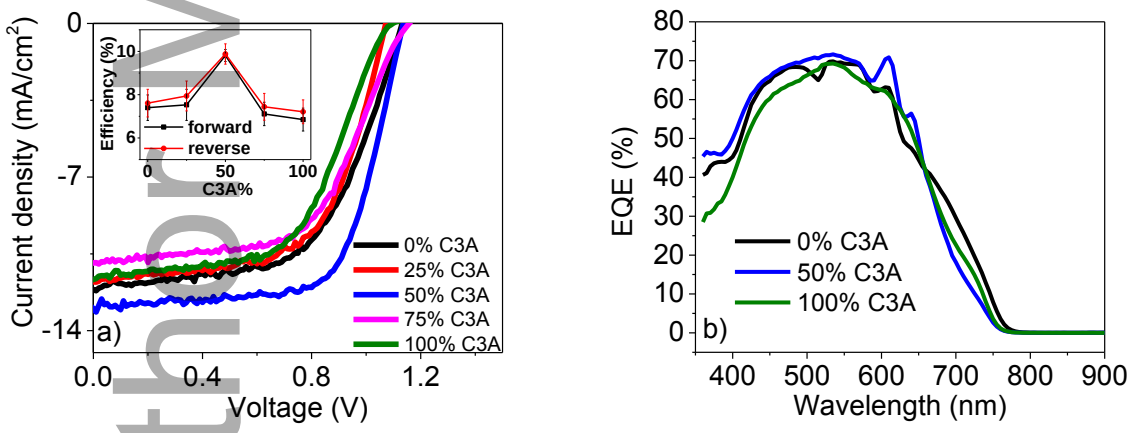

Figure 4. a) *J-V* curves of photovoltaic devices based on studied 2D perovskites; the inset is the C3A concentration dependent efficiency, and b) EQE curves of perovskite solar cells with <n>=3.

Tuning the phase composition has a strong impact on the device performance of such 2D perovskite (<n>=3) based solar cells. As summarized in **Figure 4** and **Table 1**, the selective removal of n=1 phase in the case of 1:1 mixed cation of C3A and PEA based 2D perovskites leads to appreciable improvement on the short circuit current density (J_{sc}) and fill factor (FF)

of its solar cells, reaching an overall efficiency of ~ 10%, a 30% improvement compared with the efficiency by the pure PEA based solar cells. Given that *n*=1 phase has limited absorption due to a large band gap, and slow charge transport, eliminating *n*=1 phase in the case of 50% C3A would lead to the observed enhancement of efficiency.

Table 1. Photovoltaic device performance of C3A:PEA mix cations based 2D perovskites

C3A%	scan direction	J_{sc} (mA/cm2)	V_{oc} (V)	FF (%)	η (%)
0%	forward	12.00±0.48	1.119±0.017	55.2±3.7	7.40±0.59
	reverse	11.92±0.46	1.133±0.011	56.4±4.3	7.61±0.64
25%	forward	11.25±0.74	1.071±0.047	62.4±1.2	7.53±0.72
	reverse	11.23±0.79	1.057±0.043	66.8±1.6	7.94±0.69
50%	forward	12.91±0.37	1.131±0.011	67.2±1.1	9.81±0.28
	reverse	12.86±0.31	1.122±0.014	68.5±2.8	9.88±0.47
75%	forward	11.12±0.97	1.154±0.005	55.5±1.3	7.11±0.54
	reverse	10.97±0.94	1.153±0.004	58.9±3.2	7.44±0.62
100%	forward	11.47±0.79	1.101±0.030	54.3±2.7	6.85±0.53
	reverse	11.49±0.76	1.145±0.010	54.8±2.5	7.21±0.55

As we proposed previously, the substitution of C3A into PEA based 2D perovskites could also remove defects (trap states) in the PEA based perovskite due to the small size of C3A. To verify this hypothesis, we further measured the density of trap states in our 2D perovskites (<n>=3), using the space-charge-limited current (SCLC) technique[54, 55] with a device structure of ITO/SnO_2/2D perovskite / PCBM/Bphen/Al. Specifically, the density of trap states was calculated according to **Equation 1**.

$$n_{trap} = \frac{2V_{TFL}\varepsilon\varepsilon_0}{eL^2} \quad (1)$$

where *e* is the element charge, *L* is the thickness of the film (350 nm), V_{TFL} is the trap-filled limit voltage (defined as the applied voltage at the kink point, where the current increases and becomes nonlinear), ε_0 and ε are the permittivity of vacuum and the relative permittivity of 2D perovskite, here we just use 28.8 for all 2D perovskites.[56]

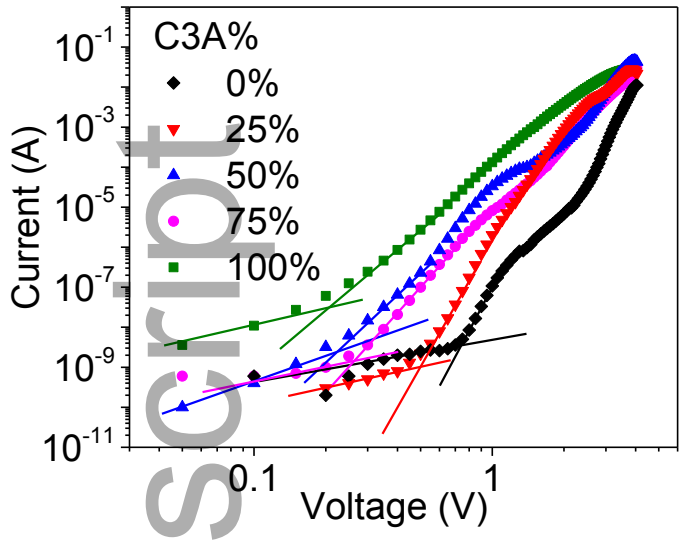

Figure 5. The trap state measurement for 2D perovskite with different C3A:PEA ratio.

Table 2. Trap state density in 2D perovskites with different C3A:PEA ratio.

C3A%	100%	75%	50%	25%	0%
V_{TFL} (V)	0.21	0.26	0.22	0.50	0.74
n_{trap} ($\times 10^{15}$ cm^{-3})	5.45	6.75	5.71	12.99	19.22

The measured dark *J-V* curves are shown in **Figure 5**, with which the extracted values of the density of trap states for these 2D perovskites are summarized in **Table 2**. Indeed, the density of trap states density monotonically decreases as the amount of C3A increases from 0% to 50%, consistent with the increasing FF. However, further increasing the amount of C3A to 75% and finally to 100% does not lead to further decrease of the density of trap states, yet the fill factor of corresponding solar cells continues to decrease. Since the fill factor of the perovskite solar cell is also affected by other factors, such as the crystal grain sizes, it is likely that factors other than defect passivation also play important roles in these 2D perovskite solar cells, in particular, for the 75% C3A based 2D perovskites (and 100% C3A, too).

2.4. Morphology of 2D perovskite films of different C3A:PEA ratio

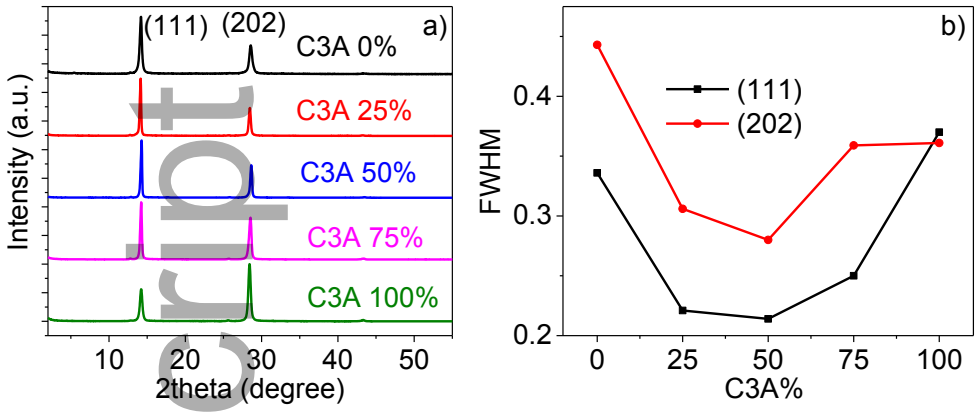

Figure 6. a) XRD of 2D perovskite films of different C3A:PEA ratio, **b)** FWHM of (111) and (202) peak from 2D perovskite films of different C3A:PEA ratio.

To probe the crystallinity and crystal grain sizes, we further investigated our 2D perovskite films (<n>=3) with XRD and AFM. For all these 2D perovskite films with different C3A:PEA ratios, we only observed strong (111), (202) peaks in their XRD patterns, as shown in **Figure 6a**, indicating highly orientated films, consistent with previous reports.[15] The 50% C3A based 2D perovskite film has the smallest full width at half maximum (FWHM), as shown in **Figure 6b**, indicating largest crystalline grain size. Further increasing the amount of C3A to 75% and 100% leads to a larger FWHM, indicating smaller crystalline grain size. Small crystalline grains would impede the charge transport, accounting for a lower fill factor in these 2D perovskite based solar cells.

The surface morphology of perovskites has a strong impact on the device performance. We first applied scanning electron microscope (SEM) to probe the surface. Unfortunately, the obtained SEM images (**Figure S6)** do not show sufficient contrast between the grain boundaries and the grains, precluding us from observing the grain size. Similar observations have been reported for 2D perovskite films in our previous study.[31] Nevertheless, we observed difference in the size and density of pinholes among these 2D perovskites films. In short, the surface morphology of the 2D perovskite film gets better as the amount of C3A increases. For example, we observed many large pinholes with 25% C3A based perovskite

film, while the 50% C3A base film showed smaller pinholes. Interestingly, 75% C3A and pure C3A based perovskite films did not show much sign of pinholes (almost pinhole-free). Thought obscured by the pinholes, we believe that the better surface morphology for 50% C3A based film also contributes to the better *FF* for 50% C3A based 2D perovskite solar cells than the ones with lower C3A amount (i.e., pure PEA and 25% C3A).

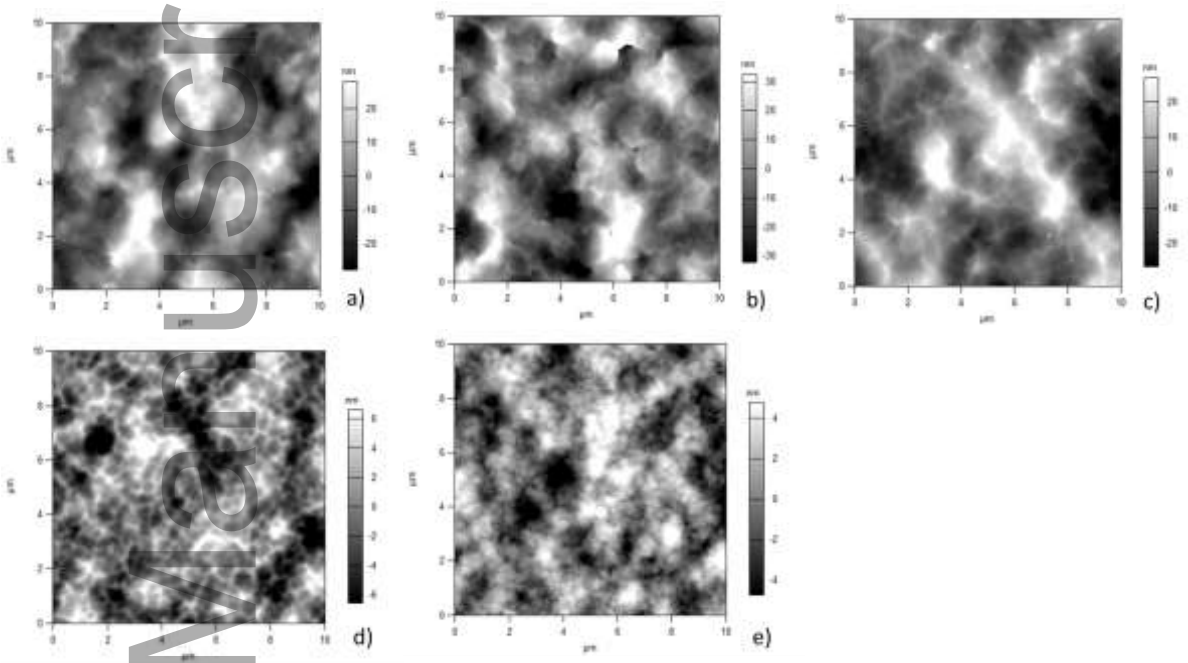

Figure 7. AFM height images of 2D perovskites of different C3A:PEA ratio: a) 0% C3A (pure PEA), b) 25% C3A, c) 50% C3A, d) 75% C3A and e) 100% C3A (pure C3A). The average roughness values are: a) 13.491 nm, b) 15.964 nm, c) 12.817 nm, d) 3.264 nm, and e) 2.352 nm, correspondingly.

Further probing the surface morphology via AFM indicates that the films of 2D perovskites with low C3A amount (i.e., 0%, 25% and 50% C3A) exhibit similar surface roughness (**Figure 7**). In contrast, the films with high amount of C3A (i.e., 75% and 100% C3A) are smoother. Furthermore, it can be observed from these AFM images that the grain sizes for the film having higher amount of C3A (75% and 100%) are visibly smaller than the ones having lower amount of C3A (0%, 25% and 50%), consistent with the trend determined by FWHM with XRD measurements.

These results point to another important factor that affects the photovoltaic device efficiency of 2D perovskites: the size of the crystalline grains. In earlier section, we

demonstrate that further increase of C3A from 50% to 75% and 100% offers similar passivation effect, i.e., low density of trap states, which would lead to similar *FF* values of the PV devices for 50%, 75% and 100% C3A based 2D perovskites; however, as we show in this section, as the amount of C3A increases from 50% to 100%, the crystal grain size in 2D perovskite films gets smaller, which would impede charge transport and result in low *FF*. For these reasons, the 2D perovskite film with 50% C3A incorporation shows the best *FF* in our study, since it has both low density trap states and large crystal grain size.

2.5. 2D RP perovskite solar cell by mixing C3A with other aromatic cations

Since the CH···π interaction should exist between C3A and other aromatic ammonium cations, we next tested whether substituting C3A into other aromatic ammonium cation based 2D perovskites would offer similar performance enhancement in their solar cells. Pleasingly, a noticeable enhancement of efficiency (and even significant in some cases) was observed for all studied aromatic cation based 2D perovskite (<n>=3) solar cells after substituting 50% C3A into the film (**Figure 8**), when compared with the pure aromatic cations based ones *and* the pure C3A based one. These encouraging results indicate that this new approach of tuning CH···π interaction could be a rather universal approach to enhance efficiency of aromatic cation based 2D perovskite solar cells.

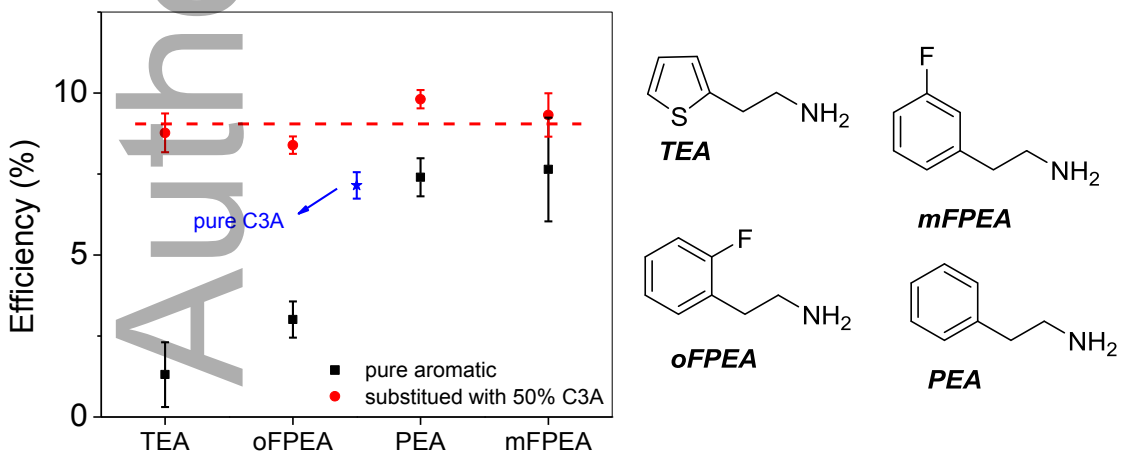

Figure 8. Photovoltaic device efficiency enhancement of 2D perovskites with <n>=3 for PEA, oF1PEA, mF1PEA and TEA after substituting 50% C3A. The chemical structures of these aromatic amines are also listed.

3. Conclusion

The CH···π interaction is a weak non-covalently interaction and often overpowered by other stronger interactions in given organic molecules; yet it can play an important role in fine-tuning intermolecular interaction in the solid state, which, as we show here, has a significant impact on the phase composition of 2D perovskites. Substituting 50% C3A into PEA based 2D perovskites can (a) selectively remove *n*=1 phase, which helps improve the film absorption and charge transport, (b) passivate the trap states, and (c) improve the morphology with larger crystalline grain size. All these contribute to the much improved photovoltaic device efficiency (~ 10%) for the 1:1 C3A:PEA based 2D perovskites (<n> =3), a 30% increase over pure PEA based ones. Since the tuning of CH···π interaction is not specific to the studied C3A and PEA, other aromatic ammonium cations can also have similar CH···π interaction with C3A and enjoy the similar benefits, leading to observed photovoltaic performance increase in these cations based 2D perovskites. The fact that all devices reaching similar level of efficiency (~ 10%), independent of the chemical nature of aromatic units and the starting device efficiency based on pure aromatic cations based 2D perovskites, implies that (a) this method could be rather universal and (b) the CH···π interaction must be the deciding underlying factor in achieving high device performance.

Supporting Information

Supporting Information is available from the Wiley Online Library or from the author.

Acknowledgements

L.Y., J.H. and W.Y. are supported by the National Science Foundation (DMR-1728921) and UNC Research Opportunities Initiative (ROI) through the Center of Hybrid Materials Enabled Electronic Technology and the Center for Hybrid Organic Inorganic Semiconductors for Energy (CHOISE), an Energy Frontier Research Center funded by the U.S. Department of Energy (DOE), Office of Science, Office of Basic Energy Sciences (BES). The FTIR, XRD, SEM and AFM in this work was performed in part at the Chapel Hill Analytical and Nanofabrication Laboratory, CHANL, a member of the North Carolina Research Triangle Nanotechnology Network, RTNN, which is supported by the National Science Foundation, Grant ECCS-1542015, as part of the National Nanotechnology Coordinated Infrastructure, NNCI. L.Y. and W.Y. thank Stephanie Samson, Sara Wehlin and Professor Gerald Meyer

(UNC-Chapel Hill) for assistance with PL measurements. N.Z. and A.M.M. are supported by National Science Foundation (CHE-1763207).

Received: ((will be filled in by the editorial staff))
Revised: ((will be filled in by the editorial staff))
Published online: ((will be filled in by the editorial staff))

References

[1] J. Hu, L. Yan, W. You, *Adv. Mater.* **2018**, 30, 1802041.
[2] G. Grancini, M. K. Nazeeruddin, *Nat. Rev. Mater.* **2019**, 4, 4.
[3] Y. Zheng, T. Niu, X. Ran, J. Qiu, B. Li, Y. Xia, Y. Chen, W. Huang, *J. Mater. Chem. A* **2019**, 7, 13860.
[4] L. N. Quan, M. Yuan, R. Comin, O. Voznyy, E. M. Beauregard, S. Hoogland, A. Buin, A. R. Kirmani, K. Zhao, A. Amassian, D. H. Kim, E. H. Sargent, *J. Am. Chem. Soc.* **2016**, 138, 2649.
[5] Y. Lin, Y. Bai, Y. Fang, Z. Chen, S. Yang, X. Zheng, S. Tang, Y. Liu, J. Zhao, J. Huang, *J. Phys. Chem. Lett.* **2018**, 9, 654.
[6] Q. Jiang, Y. Zhao, X. Zhang, X. Yang, Y. Chen, Z. Chu, Q. Ye, X. Li, Z. Yin, J. You, *Nat. Photonics* **2019**, 13, 460.
[7] W. Xu, Q. Hu, S. Bai, C. Bao, Y. Miao, Z. Yuan, T. Borzda, A. J. Barker, E. Tyukalova, Z. Hu, M. Kawecki, H. Wang, Z. Yan, X. Liu, X. Shi, K. Uvdal, M. Fahlman, W. Zhang, M. Duchamp, J.-M. Liu, A. Petrozza, J. Wang, L.-M. Liu, W. Huang, F. Gao, *Nat. Photonics* **2019**, 13, 418.
[8] K. Lin, J. Xing, L. N. Quan, F. P. G. de Arquer, X. Gong, J. Lu, L. Xie, W. Zhao, D. Zhang, C. Yan, W. Li, X. Liu, Y. Lu, J. Kirman, E. H. Sargent, Q. Xiong, Z. Wei, *Nature* **2018**, 562, 245.
[9] C. R. Kagan, D. B. Mitzi, C. D. Dimitrakopoulos, a. R. Brown, a. Pomp, C. M. Hart, D. M. D. Leeuw, S. F. Nelson, Y. Y. Lin, D. J. Gundlach, T. N. Jackson, P. T. Herwig, K. Müllen, G. Horowitz, D. Fichou, X. Peng, Z. Xu, F. Garnier, B. Furman, T. Graham, S. Hegde, S. Purushothaman, J. H. Burroughes, C. a. Jones, R. H. Friend, a. Tsumura, H. Koezuka, T. Ando, Z. Bao, a. Dodabalapur, a. J. Lovinger, C. P. Jarrett, M. Matters, R. Hajlaoui, a. Yassar, P. Srivastava, J. Kymissis, a. Callegari, J. M. Shaw, C. a. Feild, Z. Schlesinger, R. B. Laibowitz, W. T. a. Harrison, a. M. Guloy, C. Q. Xu, K. Liang, M. T. Prikas, M. Era, T. Hattori, T. Taira, T. Tsutsui, K. Chondroudis, G. C. Papavassiliou, I. B. Koutselas, a. Terzis, M. H. Whangbo, M. Shur, M. Hack, J. G. Shaw, L. Torsi, H. E. Katz, *Science* **1999**, 286, 945.
[10] D. B. Mitzi, C. A. Feild, W. T. A. Harrison, A. M. Guloy, *Nature* **1994**, 369, 467.
[11] T. Matsushima, F. Mathevet, B. Heinrich, S. Terakawa, T. Fujihara, C. Qin, A. S. D. Sandanayaka, J.-C. Ribierre, C. Adachi, *Appl. Phys. Lett.* **2016**, 109, 253301.
[12] T. Matsushima, S. Hwang, A. S. D. Sandanayaka, C. Qin, S. Terakawa, T. Fujihara, M. Yahiro, C. Adachi, *Adv. Mater.* **2016**, 28, 10275.
[13] Y. Chen, Y. Sun, J. Peng, J. Tang, K. Zheng, Z. Liang, *Adv. Mater.* **2018**, 30, 1703487.
[14] D. H. Cao, C. C. Stoumpos, O. K. Farha, J. T. Hupp, M. G. Kanatzidis, *J. Am. Chem. Soc.* **2015**, 137, 7843.
[15] H. Tsai, W. Nie, J.-C. Blancon, C. C. Stoumpos, R. Asadpour, B. Harutyunyan, A. J. Neukirch, R. Verduzco, J. J. Crochet, S. Tretiak, L. Pedesseau, J. Even, M. A. Alam, G. Gupta, J. Lou, P. M. Ajayan, M. J. Bedzyk, M. G. Kanatzidis, A. D. Mohite, *Nature* **2016**, 536, 312.
[16] A. H. Proppe, R. Quintero-Bermudez, H. Tan, O. Voznyy, S. O. Kelley, E. H. Sargent, *J. Am. Chem. Soc.* **2018**, 140, 2890.
[17] N. Zhou, Y. Shen, L. Li, S. Tan, N. Liu, G. Zheng, Q. Chen, H. Zhou, *J. Am. Chem. Soc.* **2018**, 140, 459.
[18] C. Ma, D. Shen, T.-W. Ng, M.-F. Lo, C.-S. Lee, *Adv. Mater.* **2018**, 30, 1800710.
[19] W. Fu, J. Wang, L. Zuo, K. Gao, F. Liu, D. S. Ginger, A. K. Y. Jen, *ACS Energy Lett.* **2018**, 3, 2086.
[20] J. Liu, J. Leng, K. Wu, J. Zhang, S. Jin, *J. Am. Chem. Soc.* **2017**, 139, 1432.

[21] J. Qiu, Y. Zheng, Y. Xia, L. Chao, Y. Chen, W. Huang, *Adv. Funct. Mater.* **2018**, DOI:10.1002/adfm.201806831.
[22] I. C. Smith, E. T. Hoke, D. Solis-Ibarra, M. D. McGehee, H. I. Karunadasa, *Angew. Chem. Int. Ed.* **2014**, 53, 11232.
[23] X. Zhang, X. Ren, B. Liu, R. Munir, X. Zhu, D. Yang, J. Li, Y. Liu, D.-M. Smilgies, R. Li, Z. Yang, T. Niu, X. Wang, A. Amassian, K. Zhao, S. Liu, *Energy Environ. Sci.* **2017**, 10, 2095.
[24] M. Long, T. Zhang, D. Chen, M. Qin, Z. Chen, L. Gong, X. Lu, F. Xie, W. Xie, J. Chen, J. Xu, *ACS Energy Lett.* **2019**, 4, 1025.
[25] X. Lian, J. Chen, M. Qin, Y. Zhang, T. Shuoxun, X. Lu, G. Wu, H. Chen, *Angew. Chem.* **2019**, DOI: 10.1002/ange.201902959.
[26] S. Tan, N. Zhou, Y. Chen, L. Li, G. Liu, P. Liu, C. Zhu, J. Lu, W. Sun, Q. Chen, H. Zhou, *Adv. Energy Mater.* **2019**, 9, 1803024.
[27] J. Qiu, Y. Xia, Y. Zheng, W. Hui, H. Gu, W. Yuan, H. Yu, L. Chao, T. Niu, Y. Yang, X. Gao, Y. Chen, W. Huang, *ACS Energy Lett.* **2019**, 4, 1513.
[28] X. Zhang, G. Wu, W. Fu, M. Qin, W. Yang, J. Yan, Z. Zhang, X. Lu, H. Chen, *Adv. Energy Mater.* **2018**, 8, 1702498.
[29] X. Zhang, G. Wu, S. Yang, W. Fu, Z. Zhang, C. Chen, W. Liu, J. Yan, W. Yang, H. Chen, *Small* **2017**, 13, 1700611.
[30] J. Qing, X.-K. Liu, M. Li, F. Liu, Z. Yuan, E. Tiukalova, Z. Yan, M. Duchamp, S. Chen, Y. Wang, S. Bai, J.-M. Liu, H. J. Snaith, C.-S. Lee, T. C. Sum, F. Gao, *Adv. Energy Mater.* **2018**, 8, 1800185.
[31] L. Yan, J. Hu, Z. Guo, H. Chen, M. F. Toney, A. M. Moran, W. You, *ACS Appl. Mater. Interfaces* **2018**, 10, 33187.
[32] C. Liu, W. Huhn, K.-Z. Du, A. Vazquez-Mayagoitia, D. Dirkes, W. You, Y. Kanai, D. B. Mitzi, V. Blum, *Phys. Rev. Lett.* **2018**, 121, 146401.
[33] M. C. Gélvez-Rueda, E. M. Hutter, D. H. Cao, N. Renaud, C. C. Stoumpos, J. T. Hupp, T. J. Savenije, M. G. Kanatzidis, F. C. Grozema, *J. Phys. Chem. C* **2017**, 121, 26566.
[34] J. Hu, I. W. H. Oswald, H. Hu, S. J. Stuard, M. M. Nahid, L. Yan, Z. Chen, H. Ade, J. R. Neilson, W. You, *ACS Mater. Lett.* **2019**, 1, 171.
[35] J. Hu, I. W. H. Oswald, S. J. Stuard, M. M. Nahid, N. Zhou, O. F. Williams, Z. Guo, L. Yan, H. Hu, Z. Chen, X. Xiao, Y. Lin, Z. Yang, J. Huang, A. M. Moran, H. Ade, J. R. Neilson, W. You, *Nat. Commun.* **2019**, 10, 1276.
[36] D. B. Mitzi, D. R. Medeiros, P. R. L. Malenfant, *Inorg. Chem.* **2002**, 41, 2134.
[37] Z. Xu, D. B. Mitzi, *Chem. Mater.* **2003**, 15, 3632.
[38] J. V. Milić, J.-H. Im, D. J. Kubicki, A. Ummadisingu, J.-Y. Seo, Y. Li, M. A. Ruiz-Preciado, M. I. Dar, S. M. Zakeeruddin, L. Emsley, M. Grätzel, *Adv. Energy Mater.* **2019**, 9, 1900284.
[39] M. Nishio, *Phys. Chem. Chem. Phys.* **2011**, 13, 13873.
[40] M. Safdari, A. Fischer, B. Xu, L. Kloo, J. M. Gardner, *J. Mater. Chem. A* **2015**, 3, 9201.
[41] J.-H. Im, J. Chung, S.-J. Kim, N.-G. Park, *Nanoscale Res. Lett.* **2012**, 7, 353.
[42] P. Cheng, Z. Xu, J. Li, Y. Liu, Y. Fan, L. Yu, D.-M. Smilgies, C. Müller, K. Zhao, S. F. Liu, *ACS Energy Lett.* **2018**, 3, 1975.
[43] Y. Zhang, F. Li, K.-J. Jiang, J.-H. Huang, H. Wang, H. Fan, P. Wang, C.-M. Liu, L.-P. Zhang, Y. Song, *J. Mater. Chem. A* **2018**, 6, 17867.
[44] J. M. Hoffman, X. Che, S. Sidhik, X. Li, I. Hadar, J.-C. Blancon, H. Yamaguchi, M. Kepenekian, C. Katan, J. Even, C. C. Stoumpos, A. D. Mohite, M. G. Kanatzidis, *J. Am. Chem. Soc.* **2019**, 141, 10661.
[45] R. Quintero-Bermudez, A. Gold-Parker, A. H. Proppe, R. Munir, Z. Yang, S. O. Kelley, A. Amassian, M. F. Toney, E. H. Sargent, *Nat. Mater.* **2018**, 17, 900.

[46] A. Fujii, H. Hayashi, J. W. Park, T. Kazama, N. Mikami, S. Tsuzuki, *Phys. Chem. Chem. Phys.* **2011**, 13, 14131.
[47] S. Tsuzuki, K. Honda, T. Uchimaru, M. Mikami, K. Tanabe, *J. Am. Chem. Soc.* **2000**, 122, 3746.
[48] M. J. Plevin, D. L. Bryce, J. Boisbouvier, *Nat. Chem.* **2010**, 2, 466.
[49] K.-z. Du, Q. Tu, X. Zhang, Q. Han, J. Liu, S. Zauscher, D. B. Mitzi, *Inorg. Chem.* **2017**, 56, 9291.
[50] M. Nishio, M. N. M. H. Y. Umezawa, M. Hirota, Y. Umezawa, *The CH/π Interaction: Evidence, Nature, and Consequences*, Wiley, 1998.
[51] M. Nishio, Y. Umezawa, J. Fantini, M. S. Weiss, P. Chakrabarti, *Phys. Chem. Chem. Phys.* **2014**, 16, 12648.
[52] T. Glaser, C. Müller, M. Sendner, C. Krekeler, O. E. Semonin, T. D. Hull, O. Yaffe, J. S. Owen, W. Kowalsky, A. Pucci, R. Lovrinčić, *J. Phys. Chem. Lett.* **2015**, 6, 2913.
[53] S. K. Nayak, R. Sathishkumar, T. N. G. Row, *CrystEngComm* **2010**, 12, 3112.
[54] D. Shi, V. Adinolfi, R. Comin, M. Yuan, E. Alarousu, A. Buin, Y. Chen, S. Hoogland, A. Rothenberger, K. Katsiev, Y. Losovyj, X. Zhang, P. A. Dowben, O. F. Mohammed, E. H. Sargent, O. M. Bakr, *Science* **2015**, 347, 519.
[55] J. Jiang, Z. Jin, F. Gao, J. Sun, Q. Wang, S. Liu, *Advanced Science* **2018**, 5, 1800474.
[56] A. Poglitsch, D. Weber, *J. Chem. Phys.* **1987**, 87, 6373.

The table of contents:

Propyl ammonium (C3A) is introduced into the phenethylammonium (PEA) based 2D perovskites with <n>=3. It is found that tuning CH···π interaction between organic cations can remove undesirable *n*=1 phase, lower the density of trap states, and achieve rather large crystalline grains to improve the perovskite solar cell efficeincy to ~10%. C3A with other aromatic cations shows similar improvement.

Keyword: 2D organic inorganic hybrid perovskite, solar cell, CH···π interaction

Liang Yan, Jun Hu, Ninghao Zhou, Andrew M. Moran, Wei You*

Enhancing Photovoltaic Performance of Aromatic Ammonium based Two-Dimensional Organic-Inorganic Hybrid Perovskites via Tuning CH···π Interaction

ToC figure ((Please choose one size: 55 mm broad × 50 mm high **or** 110 mm broad × 20 mm high. Please do not use any other dimensions))